Investigating the triolein/aqueous interface and *Thermomyces lanuginosa* lipase activity

Bachelor of Science Thesis

Veronika Tolevska

Supervisor

Tommy Nylander

Examiner

Peter Jönsson

LUNDS UNIVERSITET

Division of Physical Chemistry
Lund University
Lund, Sweden

October 2018

Preface

This thesis is the final part of my Bachelor's degree in the Chemistry Programme. My studies have been made from March 2018 until October 2018, at the Division of Physical Chemistry at Lund University.

I express my sincere gratitude and deep appreciation to Dr. Tommy Nylander, my supervisor, whom I share the same small hometown with and who has been extremely supportive and patient with me. I also want to extend my sincere gratitude to his research group for a positive work environment, and to Cindy Phan for being a supportive office mate.

I am highly indebted to Dr. Allan Svendsen and Novozymes for being the backbone of this project, and for providing me guidance and the opportunity to meet up and discuss the topic.

A big thank you to Peter Holmqvist for teaching me the Ganesha SAXS system, and to Ippei Furikado for teaching me the instrumentation of the Horiba ellipsometer and for guiding me at the start of my project. Even though the ellipsometer provided me daily tasks in form of new technical problems to solve, there was a delight in following the process of improving the setup of the instrument. I want to thank Christopher Ward for the 3D printed liquid cell and for helping me solve the technical difficulties. Thank you, the adminstrative staff of the Division of Physical Chemistry for the warm welcoming and for treating me well during my stay.

To my former driving instructor Joakim Johansson and the bracing Murtans Trafikskola in Falkenberg, I would like to thank for the two weeks I have spent in June getting my driving license. Those two weeks did not only reward me with a driving licence, but helped me recharge my batteries and get excited for my summer in the laboratory.

Last but by no means least, I would like to thank my family for having faith in me and loving me endlessly. You are my greatest support system.

Abstract

The triglyceride/ aqueous interface has an important role in many processes, e.g. lipase activity. Lipase is responsible for the degradation of triglycerides to smaller components, such as fatty acids. The enzyme attracts interest in industrial applications of the catalytic behavior it possesses, such as in food and pharmaceutical industries. Thus, understanding the interface which is controlling its activity, is of importance. The emulsification and the interface of triolein and water is investigated in terms of water inclusion and *Thermomyces lanuginosa* lipase (TLL) activity, to gain information about the workings of the interface and TLL relation. Based on measurements of the thickness change of a triolein film over time, using spectroscopic ellipsometry (SE), the water uptake in the triolein phase appears to increase when active or inactive TLL is present in the aqueous solution. The presence of TLL was further investigated with small angle X-ray scattering (SAXS) and wide angle X-ray scattering (WAXS), which suggested a longer repeat distance of triolein molecules when active TLL is present than if it is not. This suggests bigger aggregates are formed with more water uptake, when the triolein molecules are degraded. The obtained scattering data is preliminary. The information gained from SE unfolds a portion of the molecular interactions between TLL and the lipid/aqueous interface, by indicating different trends of thickness variations of triolein, when active TLL or inactive TLL is present.

List of Abbreviations

AOI	Angle of Incidence
DLS	Dynamic Light Scattering
GOF	Goodness of Fit
NR	Neutron Reflectivity
O/W	Oil-in-Water Emulsion
PS	Polystyrene
SAXS	Small Angle X-ray Scattering
SE	Spectroscopic Ellipsometry
SWE	Single Wavelength Ellipsometry
TCEP	Tris(2-carboxyethyl)phosphine
TG	Triglyceride
TLL	*Thermomyces lanuginosa* lipase
USAXS	Ultra Small Angle X-ray Scattering
WAXS	Wide Angle X-ray Scattering
WT	Wildtype

Populärvetenskaplig sammanfattning

Den gåtfulla gränsytan mellan lipid och vatten

Lipider är amfifila, vilket betyder att de består av en hydrofil och en hydrofob del. Vid kontakt med vatten arrangerar de sig i strukturer för att undvika oönskad interaktion. Den gränsyta som uppstår mellan vatten och lipider är intressant, eftersom den spelar en viktig roll i många processer, såsom nedbrytning av lipider med så kallade lipaser. Trots detta, finns det fortfarande en saknad förståelse för hur gränsytan fungerar och ser ut.

Vid lipid/ vattengränsytan aktiveras enzymet lipas. Bara när det interagerar med gränsytan, kan enzymet hydrolysera triglycerider till di-, monoglycerider, glycerol och fettsyror. Hur detta sker och kan effektiviseras är av intresse, då lipaser attraherar industrier, så som mat- och läkemedelsindustrin, för dess mångfaldiga katalytiska förmåga.

I detta arbete har strukturstudier gjorts av triolein/ vattengränsytan när *Thermomyces lanuginosa* lipas (TLL) är närvarande, med spektroskopisk ellipsometri och röntgenspridning vid små och stora vinklar. Ellipsometrimätningarna tyder på att trioleinfasen ökar i tjocklek över tid, när den exponeras för vatten. Dessutom ökar tjockleken när aktivt vildtyp-TLL eller inaktivt TLL finns i vattenlösningen. Men trenden för ökningen är olika för båda situationer. Den slutsats som kan tas är att lipas har en påverkan av vattenintaget i lipidfasen, och att påverkan ser olika ut för olika lipastyper. Tidigare studier indikerar att inaktivt TLL minskar lipidtjockleken vilket är i kontrast till vad som visas i denna studie. Orsakerna till denna diskrepans diskuteras.

Table of contents

1. Introduction

1.1 Aim

Lipase is a biocatalyst attractive to various industries, and thus understanding how the enzyme is operating is of importance for the optimization of industrial processes. Common for many lipases is a ”lid”, i.e. a structural domain significant for the activation of the enzyme. This trait is found in lipase from *Thermomyces lanuginosa* (TLL), which shows enhanced activity at the lipid/aqueous interface [1]. This interfacial activation plays an important role in the water inclusion of the lipid phase when in a aqueous environment. This interface is also applied to industrial systems, but also common in biological processes. In this work, the triolein/aqueous interface is investigated with ellipsometry and scattering techniques. Different types of TLL are added, such as wildtype and inactive, to see how the interface is changing in terms of enzyme activity, by investigating water inclusion and thickness variation of the triolein phase.

1.2 Theory

1.2.1 Emulsions and interfaces

A dispersion of immiscible liquids is called an emulsion, and the mixture of oil and water is the most common one. In an oil-in-water emulsion (o/w), oil is the dispersed phase and water is the continuous phase. This means there are oil droplets in an aqueous environment. Between the two phases is an interface. Interfaces are featured everywhere, i.a. in the atmosphere, human body and food. The workings of a system is sometimes altered by the interface. Accordingly, understanding the interface is important when explaining a system.

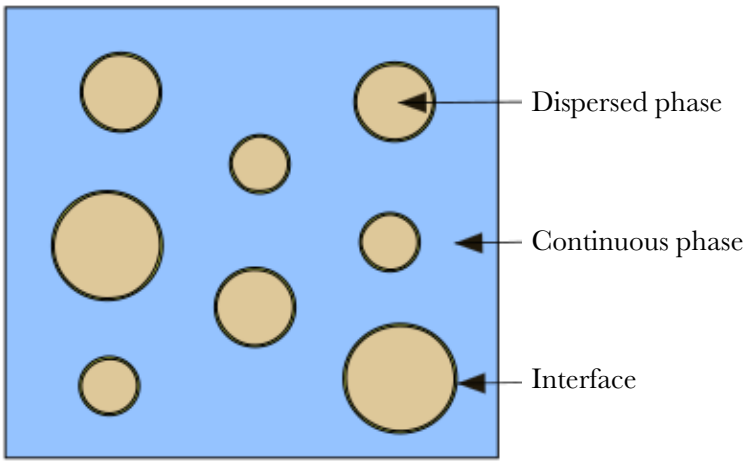

Figure 1. Oil-in-water emulsion. The brown spheres are oil droplets and the surrounding blue is water.

The contact between oil and water molecules is thermodynamically unfavorable. Thus the formation of an emulsion is generated by dispersion and condensation methods, such as mechanical stirring and an emulsifier is often added to obtain a stable emulsion [2]. Emulsifiers are additives that position themselves at the interface of the two phases, to reduce the interfacial tension between the oil and water. An emulsion is metastable because of its kinetic instability, i.e. the phases will separate after a period of time (see figure 2).

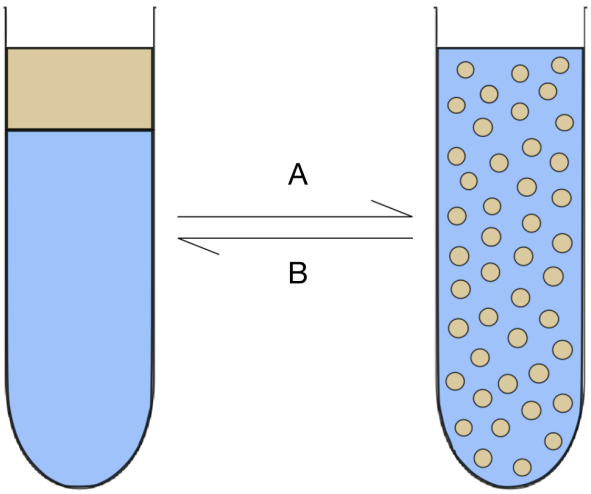

Figure 2. Left: oil and water phase separated. Right: oil-in-water emulsion. The o/w is achieved by e.g. stirring (A) and the phase separation is achieved by e.g. waiting (B).

1.2.2 Lipids

Lipids are amphiphilic, with a hydrophilic head and a lypophilic tail of hydrocarbons. In o/w, the tails are oriented in a way to avoid contact with the aqueous environment, which only the lipid heads are facing [3]. This self-assembled aggregate varies in structure, depending on the volume and length of the hydrophobic part and the area of the hydrophilic head group [4]. The aggregation is driven by i.a. the hydrophobic effect [5].

Triolein is a lipid with three units of a hydrophobic hydrocarbon tail. The tails are derivates of oleic acid, and the head is derivated glycerol. Thus, triolein is referred to as a triglyceride (TG).

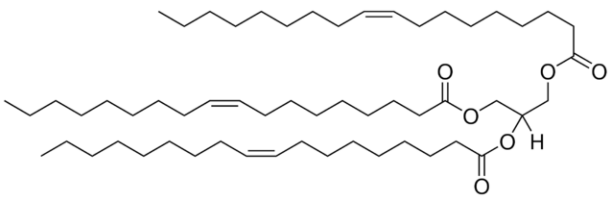

Figure 3. The structure of triolein [6]

The hydrophobic part of the triolein molecule is bulky, since it consists of three unsaturated hydrocarbon chains. The kinks caused by the double bonds will prevent the molecules from being densely packed. Hence, the structure of the formed aggregates are rather complex. In contrast, phospolipids are mainly forming bilayer structures, which in polar solvent, can be stacked on each other with aqueous films in between. This is the generic packing of a lamellar phase, such as liquid crystalline and gel phase [4].

1.2.2.1 The E-type and F-type conformation of triolein in aqueous solution

An aggregate of triolein molecules does not consist in the conformation illustrated in figure 3, since it is not considering the complicacy of the structure. In a three dimensional polymorphic form, the triolein molecule undergoes a tuning fork conformation, also known as the F-type, in which one chain is facing the opposite direction than the other two chains (see figure 4). The second conformation triolein can undergo is of E-type, in which all the hydrocarbon chains point in the same direction (see figure 4).

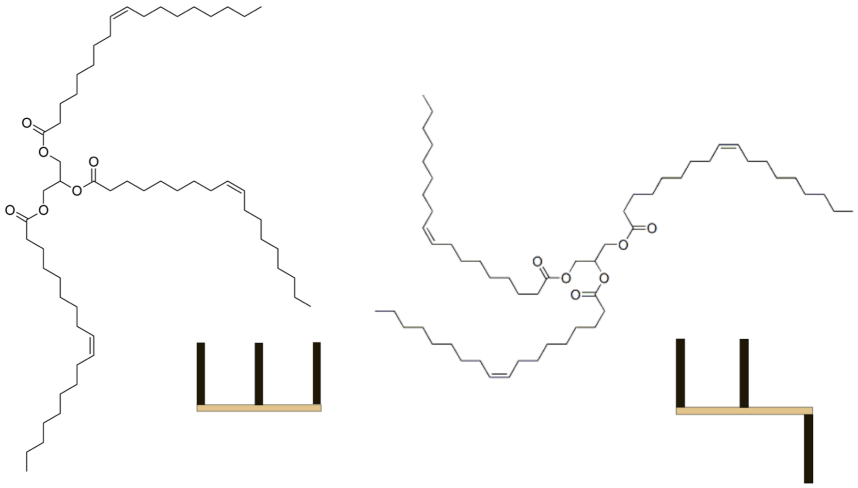

Figure 4. From left to right: the E-type conformation and F-type conformation of triolein [7, 8]

The F-type is preferred in a three dimensional polymorphic form, since there is more of a steric hindrance in the E-type conformation. In the condenced phase, a triolein monolayer facing water consists of molecules in the E-type conformation. The stabilization of E-type is presumably hydrogen bonding between the carbonyl groups of the glyceryl head group and the water molecules [9]. Contrarily, in multilayers of triolein, the E-type is only favorable in the layer at the interface with water. The outer layer consists of triolein molecules in the F-type conformation [10, 11, 12].

1.2.3 Lipases

Lipase is a hydrolase, i.e. an enzyme that catalyses the hydrolysis of ester bonds. The enzyme degrades triglycerides into di- and monoglycerides, glycerol and fatty acids [13]. The lypolytic enzyme targets ester bonds for degradation. Its activity is enhanced at the interface of water and lipid. As mentioned, the carbonyl groups of the polar head of triolen is facing the aqueous solution. The same interfacial alignment is applicable for generic TGs, and lipase is activated by it, which is the phenomenom described as interfacial activation [14].

1.2.3.1 The interfacial activation of *Thermomyces lanuginosa* lipase

Lipase from *Thermomyces lanuginosa* (TLL) has a ”lid”, consisting of protein residues 82-89, that plays an important role in the activation of the enzyme. At the triolein/ aqueous interface, TLL undergoes a conformational change. The lid region is dislocated to expose the catalytic triad of S146, H258 and D201 [15]. The dislocation of S83 for example, enables bonding of NH between the substrate and lipase, and a nucleophilic attack happens on the scissile ester bond which initiates the hydrolysis of the substrate [16, 17]. Mutations in the lid region can prevent the change in conformation, thus the lid differs between wildtype and the inactive forms of TLL. In this experiment, the inactive TLL (S146A) and locked TLL (C86C255) have mutations inside the catalytic triad and inside the lid region, respectively. The mutation in the inactive TLL is a substitution of S146 with alanine (A) [18]. A hydrophobic interaction is present between I86 and neighbouring I255, and it is broken when the lid is opening. The locked TLL has cysteine residues at these positions, disulfide bonded to each other, which do not break at the interface and thus prevent the lid from opening. Therefore, no lipolytic activity is present [9]. Tris(2-carboxyethyl)phosphine (TCEP) is a bulky reducing agent, which in the right concentration, reduces the disulfide bond between C86 and C255 [19].

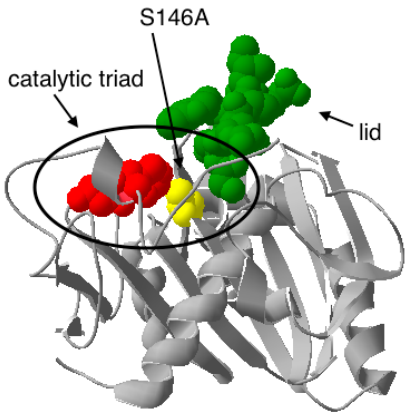

Figure 5. A picture of inactive TLL (PDB: 1GT6), viewed with Swiss PDBViewer V 4.1.1. The catalytic site is space filled and circled, where an arrow is indicating where the mutated S146A is located. The other space filled region is the lid of TLL. S146A is rather enclosed from the surface, by the lid, in the inactivated form of the enzyme.

1.2.4 Spectroscopic Ellipsometry

Ellipsometry is a technique for studying thin films and surfaces. The thickness and optical properties of a film are characterized from the change of polarization when a beam is reflected onto it. These are calculated quantities, model-based from the measured parameters phase shift (Δ) and amplitude ratio (Ψ).

Polarized light with an electric field oscillating parallel to the plane of incidence is called p-polarized light. The light with an electric field oscillating perpendicular to this, is s-polarized. When combined, equal in phase, these light beams can form a linearly polarized light beam. In ellipsometry, linearly polarized light is emitted and reflected onto the sample. The p- and s-polarized light components are reflected differently, and thus fall out of phase when hitting the sample. The shift in phase and amplitude make the reflected light elliptically polarized. This change of polarization state is measured as the complex reflectance ratio, p, and is dependent on the thickness and optical properties of the sample. The fundamental equation of ellipsometry is denoted as below:

$$\rho = \frac{R_p}{R_s} = tan\psi e^{i\Delta} \tag{1}$$

where ρ is the ratio of R_p and R_s, the amplitude of p- and s-polarized light respectively.

Single wavelength ellipsometry (SWE) utilizes a monochromatic light source, usually a laser at 632.8 nm, while spectroscopic ellipsometry (SE) employs multiple light sources covering a spectral range [20]. Consequently, SE provides more information

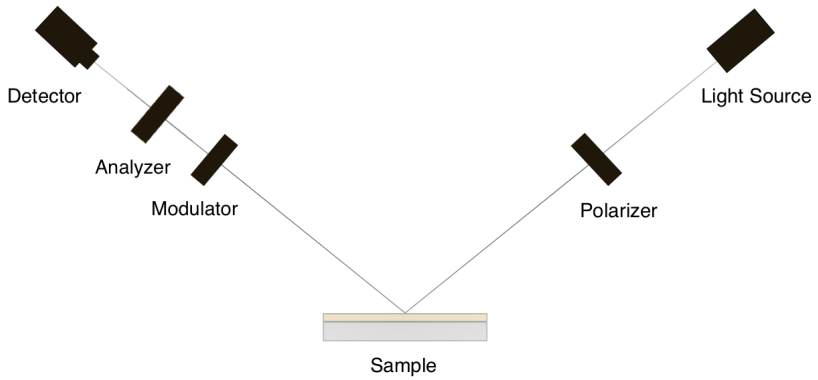

Figure 6. Schematic setup of a SE experiment

The instrumentation of spectroscopic ellipsometry consists of a light source emitting electromagnetic radiation, which is polarized linearly by a polarizer. The polarized beam reflects onto the sample and passes a modulator. The modulator changes the polarization state of the elliptically polarized beam. Straight after the modulator sits the analyzer which is a second polarizer. At last, the beam reaches the detector [21].

1.2.5 Small Angle X-ray Scattering

Structural properties of particle systems are investigated with a scattering technique known as Small Angle X-ray Scattering (SAXS). The particle systems can be solid, liquid or dispersions of colloidal particles or macromolecules.

X-rays are electromagnetic waves that pass through, get absorbed or scatter when they encounter with matter. When this radiation is scattered coherently, i.e. changed in direction and not in wavelength, it is called Rayleigh or Thomson scattering [2]. This form of elastic scattering is analyzed in SAXS, at angles of 0.1° to 10°. Analyzes at smaller angles or larger angles can be done with Ultra Small Angle X-ray Scattering (USAXS) and Wide Angle X-ray Scattering (WAXS) respectively [22].

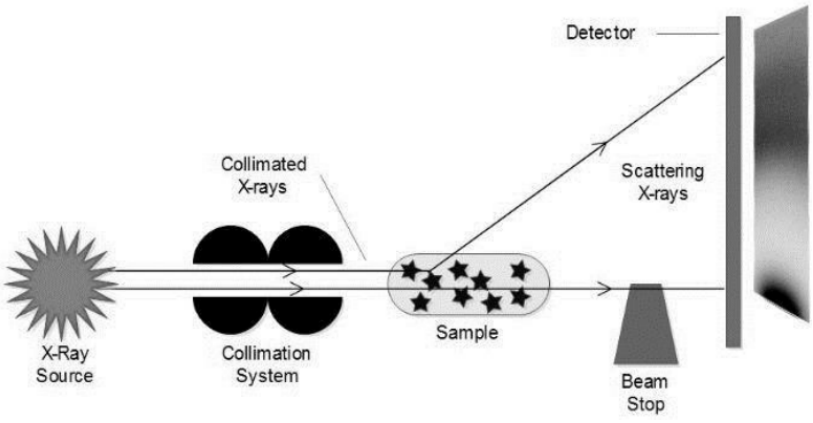

Figure 7. Schematic representation of an X-ray scattering instrument [23]

An X-ray tube with the construction of electrons hitting an anode, making the electrons decelarate and cause the emission of X-rays, is the initial component of a SAXS instrument. Connected to this, is the collimation system. The two main systems are of slits and pinholes respectively. Line collimation instruments have slits making the beam one dimensional, and thus a long and narrow line. Point collimation instruments have a beam that is a small circular or elliptical spot, which is the result of having pinholes. One dimensional or circular, the beam is hitting the sample which is in a specific chamber, where vacuum is necessary to attain low background scattering. The final component is the detector. To prevent the sample from being overshadowed by the backscatter from the material of the detector, the beam goes through a beam stop before reaching the detector (see figure 7).

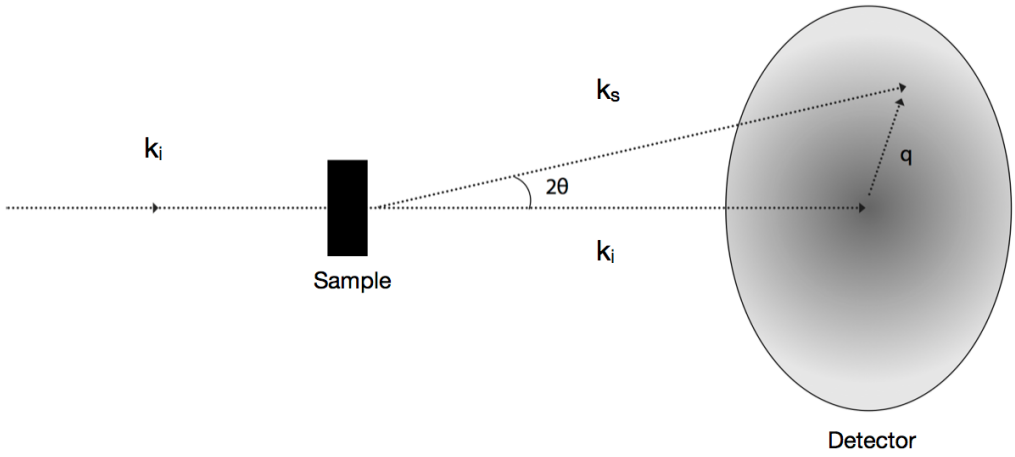

Figure 8. Schematic representation of X-ray scattering

The difference between the incident X-ray beam, k_i, and the scattered X-ray beam, k_s, is referred to as the scattering vector, q (nm^{-1}). The scattering intensity is dependent on the scattering angle, 2θ, is measured against q, and gives information about the composition of the sample. The scattering resulted from the shape and size of a particle is defined as the form factor P(q). Structural information, such as how the particles are organized in relation to one another, is given by the structure factor S(q).

When X-rays are scattered on a crystal plane, the angle of the diffracted beam is the same as the angle of the incident beam. If two X-ray beams hit a point on different lattice planes of the crystal, and have the same path difference, constructive interference and maximum intensity have occured. This condition can be expressed by Bragg's law, and it is written as follows:

$$n\lambda = 2d\ sin\theta \quad (2)$$

where n is an integer, λ is the wavelength of the radiation, d is the spacing between lattice planes and θ is the glancing angle [24]. Derivated from this, is the following equation:

$$d_{Bragg} = \frac{2\pi}{q_{Peak}} \quad (3)$$

By means of Equation 3 and obtained SAXS data, the distance between lattice points also called the repeat distance, d_{Bragg} can be calculated by extracting the scattering vector for the maximum peak, q_{peak}.

Electron density difference between particle and matrix material, e.g. the solvent, affects the intensity of the scattering signal. If the electron density of the particles is different from that of the matrix, the particles can be distinguished from the background. This is due to the arise of contrast and absorption losses are reduced [22].

2. Materials and methods

2.1 Buffer preparation

The buffer was prepared with 1 mM $CaCl_2$, 100 mM TRIS and MilliQ water. The buffer solution was adjusted with HCl (35% fuming) to pH 7.5, with the help of a pH meter and a magnetic stirrer. The final buffer solution was stored in the fridge, and was replaced if older than 1 week.

Several buffer solutions were prepared with different types and concentrations of TLL. Wildtype TLL, inactive TLL (S146A) and locked TLL (C86C255) were added to separate 100 mL glass bottles with buffer solution. Two sets of solutions were prepared, with the lipase concentration of 2 ppm and 20 ppm respectively. A buffer solution of activated TLL was prepared by adding 5 mM TCEP to a solution with locked TLL. The lipase buffer preparation is based on (Stamm et al., 2017; Skjold-Jørgensen et al., 2014 ; Skjold-Jørgensen et al., 2016) [25, 26, 27].

2.2 Spectroscopic Ellipsometry

2.2.1 Sample preparation

Hydrophilic and polished 1 x 0.7 cm^2 silicon wafers, SiO_2 coated by thermal oxidation, were used. A layer of polysterene (PS) was added on a wafer by spin coating 35 µL polysterene (0.75% in toluene) 5s at 2000 rpm. Thereafter, the wafer was spin coated with 40 µL triolein (5 mM in hexane) in the following sequence; 5 s at 2000 rpm, 5 s at 4000 rpm and 20 s at 8000 rpm. The coated wafers were put in the freezer over night.

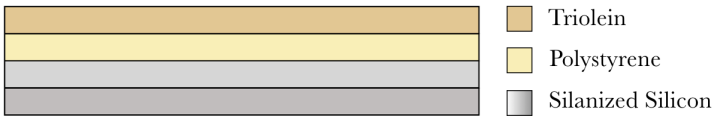

Figure 9. The layering of a silica wafer sample, where the silicon dioxide and polystyrene layer has a thickness of 300 Å, with a standard deviation of ± 10 and ± 20 Å, respectively. The triolein layer is 500-1400 Å. This is the composition used in (Stamm et al., 2017; Skjold-Jørgensen et al., 2014; Skjold-Jørgensen et al., 2016), and is used in this experiment for the possibility to compare results.

2.2.2 Cleaning procedure

The silica wafers were rinsed with ethanol, N_2 dried and put in the plasma cleaner for 10 minutes. After measurement, the wafer was cleaned for reuse by ultrasonic cleaning (Branson 2510), 10 minutes in a tube with ethanol with following 5 minutes in acetone. Thereupon, it was rinsed with ethanol and N_2 dried.

2.2.3 Setup

The ellipsometry measurements were performed on a HORIBA UVISEL-ER-AGAS Spectroscopic Ex-Situ Ellipsometer. A 3D-printed liquid cell of stainless steel was used for the interface measurements. The spectral range was set to 250-770 nm, and the integration time to 1000 ms. The angle of incidence (AOI) was 70°, modulator angle 0° and analyzer angle 45°.

The software DeltaPsi2, V 2.9 by HORIBA Jobin Yvon, was used to extract the thickness value of the triolein layer. A model of the interface was made by measuring every layer of the wafer gradually, starting with a bare silanized silicon wafer. The goodness of fit (GOF) between model and experimental data was evaluated as χ^2, the GOF parameter. The smaller the GOF parameter is, the better is the fitting. For the transparent polystyrene and triolein films, Cauchy's equation was applied as the relationship between refractive index and wavelength.

The frozen wafer with the polystyrene and triolein layer as shown in figure 9 was put in a liquid cell. Lipase buffer was added with a flow rate of 0.5 mL/ min, from a 60 mL syringe connected to a pump. The lipase buffer was added into the cell in two different ways. One way was by adding 2 ppm lipase buffer constantly for two hours. The other method was adding buffer solution for 1 hour, and then let buffer solution with lipase run through for 1 hour. A 1 hour measurement of 20 ppm wt TLL and 20 ppm S146A TLL respectively, was also performed in the same manner as the former. Measurements were conducted at room temperature (22°C), with an interval of 20 seconds.

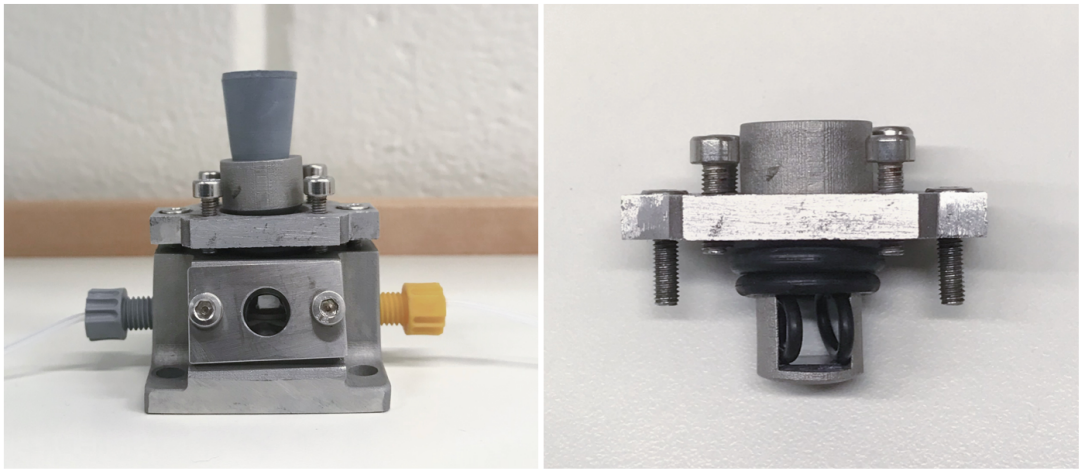

Figure 10-11. Liquid cell of stainless steel, used for the triolein/ aqueous interface measurements. It holds ca 2 mL solvent and the sample was held in place by two O-rings.

2.3 Small Angle X-ray Scattering

2.3.1 Sample preparation

A set of 6 samples were prepared with the composition explained in table 1. The five samples containing buffer were sonicated before lipase addition, until they became turbid, with pulses of 10 s, a cooling period of 10 s and an amplitude of 70%. During the sonication, the samples were in an ice bath. Subsequently, lipase was added in the concentration of 20 ppm, and the final samples were put on a roller mixer to equilibrate before measurement.

Table 1. *The preparation of 8 mL samples for SAXS measurement. The composition of all samples containing buffer, was 90% buffer and 10% triolein. In addition, a sample of only buffer was measured as matrix.*

Sample	Buffer (mL)	Triolein (mL)	Lipase
1	0	0.8	-
2	7.2	0.8	-
3	7.2	0.8	wt TLL
4	7.2	0.8	S146A TLL
5	7.2	0.8	C86C255 TLL
6	7.2	0.8	C86C255 TLL +TCEP

The samples for the WAXS measurement were prepared in the same manner, but without sonication and with 2 ppm lipase instead of 20 ppm. After the equilibration on a roller mixer, the triolein phase of a sample was collected and put in a capillary for measurement.

2.3.2 Setup

SAXSLAB's GANESHA 300XL is a SAXS instrument with pinhole system, and was used for the scattering measurements. Two pinholes were employed, and the configuration was 24 ($0.003 < q\ [Å^{-1}] < 0.22$) for the SAXS measurements, and 21 ($0.1 < q\ [Å^{-1}] <$

2.75) for the WAXS measurements. Every sample was measured for 3 hours at 25°C. The obtained data was visualized and processed with the SAXSGUI software.

3. Results and discussion

3.1 The Spectroscopic Ellipsometry measurements

3.1.1 Thickness variation of triolein during 2 hours of lipase buffer exposure

The layer of triolein on a polystyrene coated silica wafer was affected by the aqueous environment and the lipase addition, and it is shown in figures 12-14.

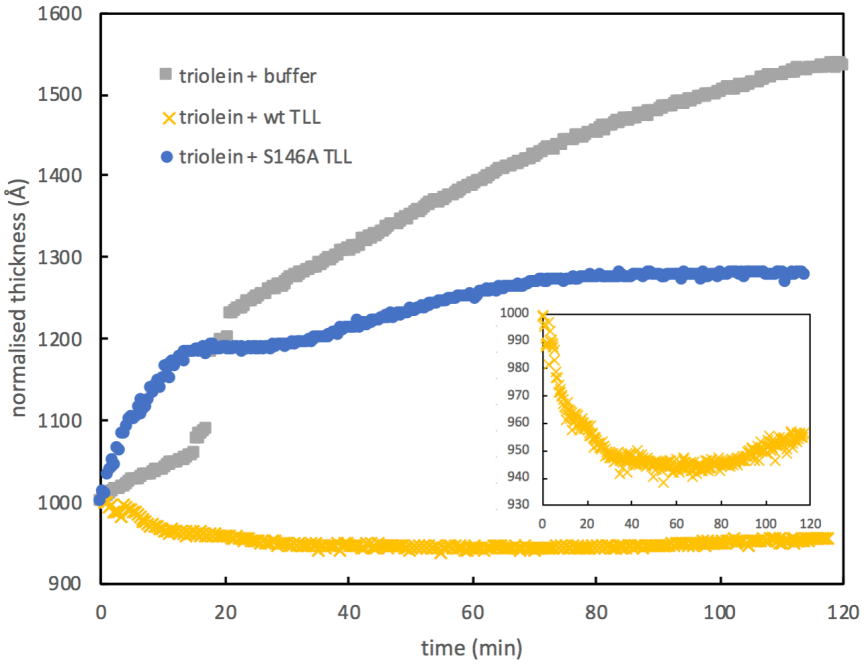

Figure 12. The thickness variation of a triolein layer over 2 hours. The thickness values are normalised from an initial thickness of 1000 Å. The standard deviation of the obtained data is ± 45 Å. The triolein thickness when exposed to buffer (squares), buffer with 2 ppm wildtype TLL (crosses) and buffer with 2ppm inactive S146A TLL (dots) are shown. The buffer has pH 7.5 and consists of 100 mM TRIS and 1 mM $CaCl_2$. The inset shows the dip of triolein layer thickness when active wildtype TLL is at the interface.

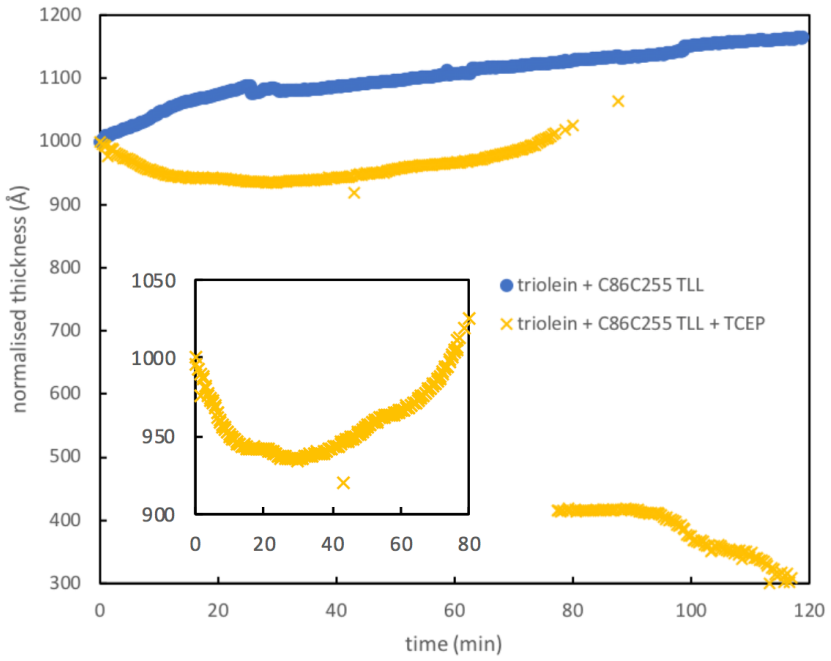

Figure 13. The thickness variation of a triolein layer over 2 hours. The thickness values are normalised from an initial thickness of 1000 Å. The standard deviation of the obtained data is ± 45 Å. The triolein thickness when exposed to a buffer with 2 ppm locked C8C255 TLL (dots), and with added 5 mM TCEP (crosses) are shown. The buffer has pH 7.5 and consists of 100 mM TRIS and 1 mM $CaCl_2$. The inset shows the dip of triolein layer thickness when active C86C255 TLL is at the interface.

The thickness is increasing for triolein exposed to buffer, as well as for triolein exposed to buffer with S146A TLL (see figure 12). The former has an instant thickness increase of approximately 100 Å at 20 minutes. At this point, the GOF parameter did not change so much, which indicates that the layer has changed. The same investigations done by (Stamm et al., 2017) with 1 hour measurements using a 20 mL flow cell in plastic, show that the triolein thickness decreases over time, when S146A TLL is present. The discussed reason for the decrease was the inactive TLL covering the interface and hindering water uptake. The hindering of the water uptake is letting the film rupture act alone, with no lypolytic activity overshadowing the decrease that the rupture of the film is causing during all measurements. In contrast, figure 12 shows that the triolein thickness was increasing considerably the first 20 minutes, and had a constant value of 1300 Å after approximately 70 minutes of thickness increase. Lipase interacts well with plastic and glass, thus loss of lipase is to be considered during the ue of pipettes, beakers, syringes and O-rings. There might have been a deficient amount of lipase present, thus the increase could be representing the condition of having less or no lipase in the system.

The thickness increase of triolein exposed to S146A TLL is 278 Å, and do not differ much from the 200 Å increase for triolein exposed to C86C255 TLL. There is an instant and large thickness decrease just before 80 minutes, of the layer exposed to a buffer solution with C86C55 TLL and TCEP (see figure 13). After 77 minutes, the GOF parameter is decreasing from 30 to 3 as the thickness is decreasing. Thus, the values are not relative to each other. The reason for this could be the layer is being washed away, and there is less substrate to measure of, which makes the fit of the single lipid layer to the model better.

Before the reduction, the triolein thickness is greater than the initial thickness value. With wildtype TLL present, there is a similiar trend in thickness variation as when C86C255 TLL is present and activated, except that the layer does not pass the initial value of 1000 Å when increasing during the same time frame. The decrease for when the active form of TLL is present, could be due to the hydrolysis happening and chunks in form of di-, monoglycerides, glycerols and fatty acids leaving the surface and the film becoming thinner. The later increase, at 80 minutes with wildtype TLL and at 30 minutes with activated C86C255 TLL, is the enhanced water uptake in the lipid layer as it becomes more polar due to the lypolysis.

3.1.2 Thickness variation of triolein during 2 hours of buffer exposure, with added lipase after 1 hour

Measurements with added wildtype TLL, inactive TLL and locked TLL respectively, mid measurement, were performed. During data evaluation, a good fit between data and model was harder to achieve than for previous measurements. The spectral range was shortened during evaluation, to lower the GOF-parameter, but the thickness values showed a great fluctuation following no trend. The interest in knowing the thickness variation, when lipase is added after one hour of buffer solution flowing through the cell, is to see how the lipase activity affects the triolein layer thickness when the layer already has taken up water for one hour.

3.1.2 The TLL concentration dependence of triolein thickness

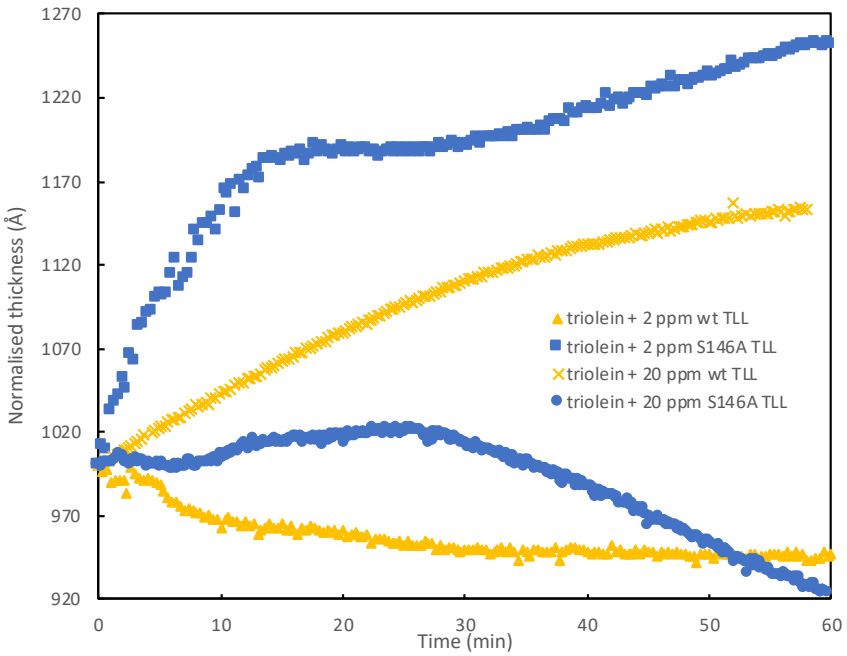

Figure 14. The thickness variation of a triolein layer over 1 hour. The thickness values are normalised from an initial thickness of 1000 Å. The standard deviation is ± 45 Å for the 2 ppm TLL measurements, and ± 60 Å for the 2 ppm TLL measurements. The triolein thickness when exposed to buffer with 20 ppm wildtype TLL (crosses), buffer with 2 ppm wildtype TLL (triangles), buffer with 20 ppm inactive S146A TLL (dots) and with 2 ppm inactive S146A TLL (squares) are shown. The buffer has pH 7.5 and consists of 100 mM TRIS and 1 mM $CaCl_2$.

The measurement of triolein layer thickness during 1 hour of 20 ppm S146A TLL buffer exposure, shows that the layer thickness decreases by approximately 100 Å as in the 1 hour experimen with 2 ppm S146A TLL, by (Stamm A. et al., 2017). The difference is the slight increase of 20 Å, during the first 25 minutes. Later, a linear decrease of the triolein thickness is visible, which correlates with the results in (Stamm A. et al., 2017). This experiment differ by having an initial thickness increase, and it could be due to the S146A TLL concentration being 10 fold the concentration of 2 ppm in (Stamm A. et al., 2017). The thickness increase when triolein is exposed to 2 ppm S146A TLL, could be equivalent to the initial increase of triolein when exposed to 20 ppm S146A TLL (see figure 14). The initial thickness increase could be the lipase saturating the layer making it appear thicker, and due to no developed lypolytic attack, the thickness starts to decrease by reasons that have already been discussed. The increase of the triolein layer when 20

ppm wildtype is present, could be the faster saturation of TLL on the film, hindering chuncks of fatty acids to disappear from the layer.

3.2 The SAXS and WAXS measurements

3.2.1 SAXS

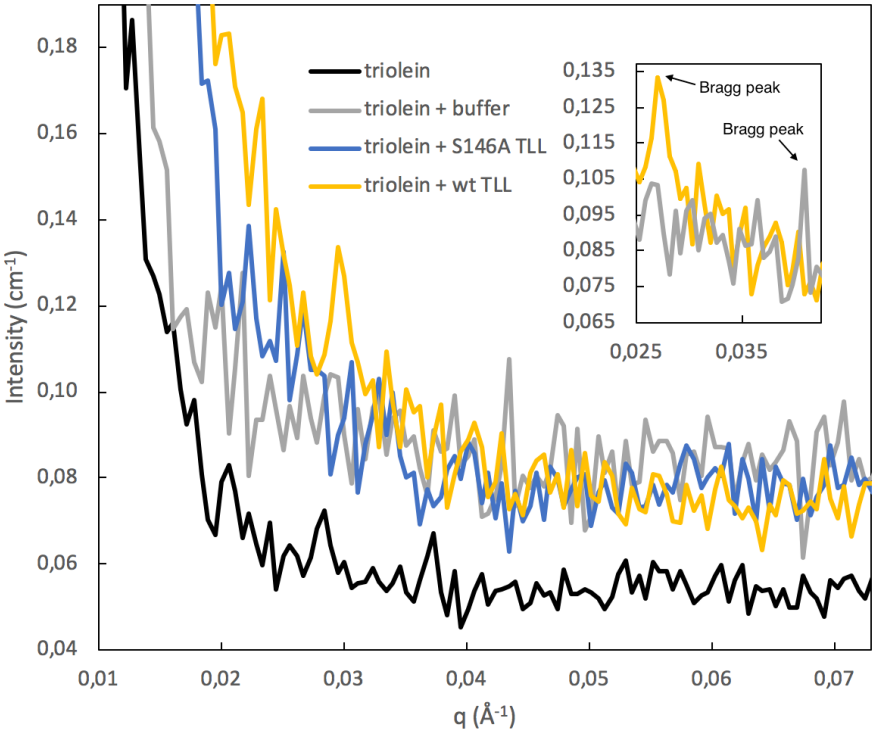

Figure 15. Intensity as a function of scattering vector. Data for triolein (black), triolein sonicated with buffer solution (grey), triolein with buffer solution containing 20 ppm inactive S146A TLL (blue) and 20 ppm wildtype TLL (yellow). The inset shows the Bragg peaks for triolein exposed to wiltype TLL (yellow), and for triolein mixed with buffer (grey). The buffer has pH 7.5 and consists of 100 mM TRIS and 1 mM $CaCl_2$.

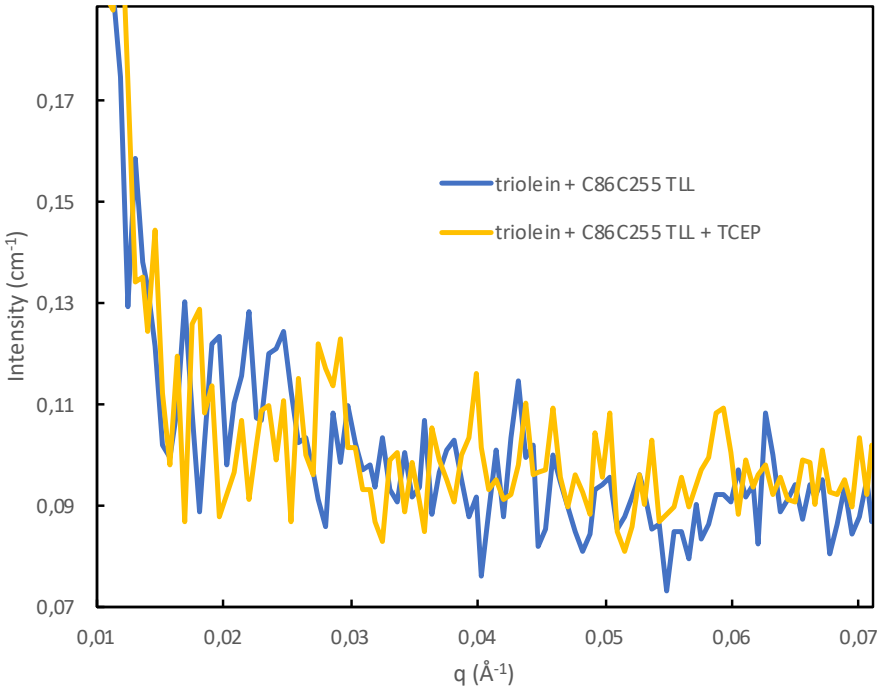

Figure 16. Intensity as a function of scattering vector. Data for triolein mixed with buffer solution containing 20 ppm locked TLL (blue), and 20 ppm locked TLL with added TCEP (yellow). The buffer has pH 7.5 and consists of 100 mM TRIS and 1 mM $CaCl_2$.

The collected SAXS data is noisy due to the insufficient sensitivity of the used instrument, possibly contributed from the weak substitute vacuum pump giving out a higher pressure than optimal. In addition, the buffer solution was never measured, due to time constraint, and thus no background subtraction was made. Therefore, no predictions can be made on what type of phases are formed. The major potential Bragg peak for triolein exposed to wildtype TLL was found at 0.0265 $Å^{-1}$, corresponding to a repeat distance of 237 Å as calculated with equation 3. The major potential Bragg peak was found for the triolein phase exposed to only buffer solution, at 0.0405 $Å^{-1}$ (see figure 11). The calculated repeat distance is 155 Å. These peaks were chosen with uncertainty, due to not being distinctive enough. The calculated values suggest that the distance between triolein molecules is greater when wildtype TLL is present than if it is not. This could be due to the triolein molecules being degraded to minor components, and larger aggregates forming, suggesting more water inclusion than if the triolein molecules were not degraded.

In contrast, (Stamm A. et al. 2017) reports a repeat distance of triolein exposed to water as 310 Å. This is twice the distance extracted from the Bragg peak in figure 14. The deviation could be due to the sonication that gives smaller oil droplets, which is not a part of the sample preparation in (Stamm A. et al. 2017).

3.2.2 WAXS

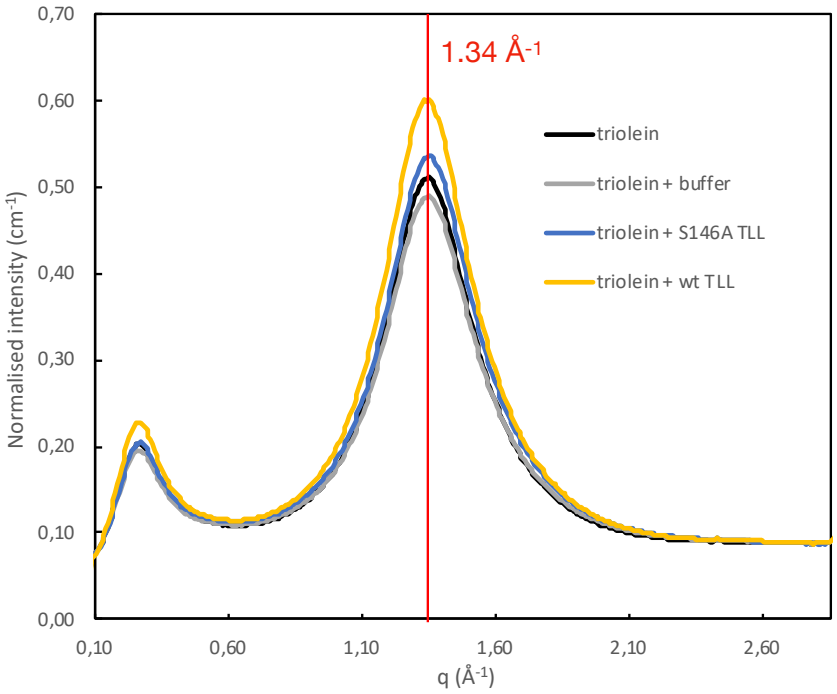

Figure 17. Intensity as a function of scattering vector. Data for triolein (black), triolein mixed with buffer solution (grey), triolein with buffer solution containing 2 ppm inactive S146A TLL (blue) and 2 ppm wildtype TLL (yellow). The red line crosses the Bragg peaks. *The buffer has pH 7.5 and consists of 100 mM TRIS and 1 mM $CaCl_2$.*

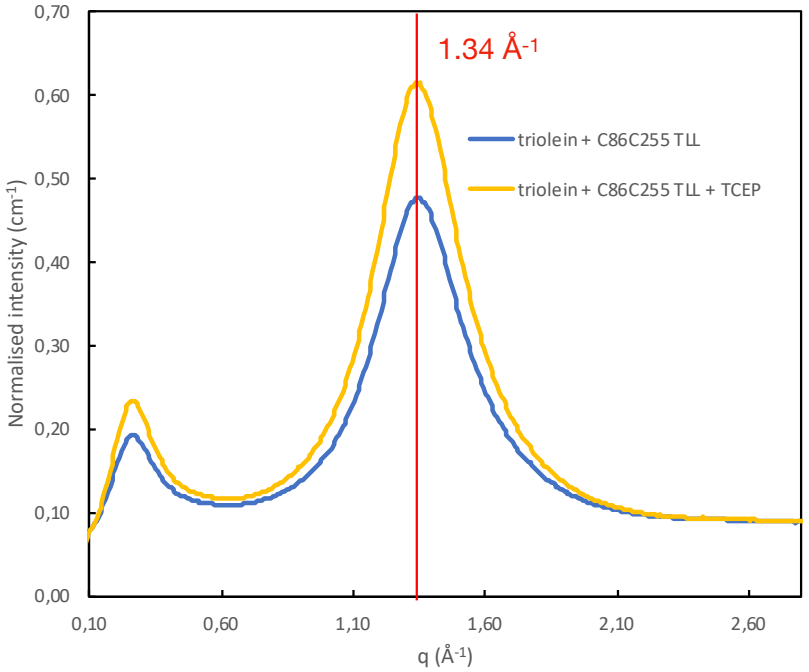

Figure 18. Intensity as a function of scattering vector. Data for triolein mixed with buffer solution with 2 ppm locked C86C255 TLL (blue) and with added 5 mM TCEP (yellow). The red line crosses the Bragg peaks. The buffer has pH 7.5 and consists of 100 mM TRIS and 1 mM $CaCl_2$.

Two intensity peaks were evident for all samples, on nearly the same q-values. From the Bragg peaks, at 1.34 $Å^{-1}$, a repeat distance of 4.69 Å is calculated. This represents the chain packing of the triolein molecules in the liquid state. On the other hand, a difference in intensity between the bulk mixtures is visible. For the triolein phase exposed to active TLL, wildtype TLL and C82C255 TLL with TCEP, the intensity is higher than for the triolein phase exposed to the inactive forms of TLL, S146A TLL and C82C255 TLL (see figure 17-18. Furthermore, the intensity is higher for triolein than for triolein mixed with buffer. This reflects the arrangement of triolein molecules. A high intensity is shown for a more structured arrangement. This means that the triolein molecules become more unstructured in buffer dispersion, and more structured when active TLL is present in the buffer solution. This implies that degraded triolein molecules are more structurally arranged.

The triolein molecules are in the E-type conformation at the interface between the dispersed triolein droplets and the continuous phase. i.e. the buffer solution. This means that the lipid molecules experience a transformation of the conformation, presumably from F-type to bulky E-type. The hydrolysis of the triolein molecules ester bonds, by wildtype TLL and activated C86C255 TLL, will result in a solution constisting of fatty acids, monoglycerides, diglycerides and glycerols. These components pack themselves in a more structured arrangement. Which phase this arrangement is representing, can not really be evaluated from the data.

3.3 Outlook

3.3.1 The lipase buffer solution

The lipase activity is not only controlled by the lipid/ aqueous interface. The dielectric constant of the solvent also affects the conformational change of the lipase. Ca^{2+} ions are included in the aqueous system to rigidifiy and order the triolein layer, since the lipids and the divalent cations are able to form intermembrane complexes that induce phase changes as documented by (Dluhy et al., 1983) [28, 29]. This way, the calcium ions also keep the dielectric constant low at the interface which trigger the lid to open more, as investigated by (Skjold-Jørgensen et al., 2015) [30]. The composition of the buffer solution

is therefore suitable for measurement of an active TLL, and it has been proven that the enzyme works efficiently at pH 7-8, by (Skjold-Jørgensen et al., 2014) [26].

Too much of the agent TCEP may reduce not only the targeted bond between C86 and C255, but natural disulfide bonds in the lipase as well. Underlying enzymatic activity studies by (Skjold-Jørgensen J. et al., 2017), shows that 5mM TCEP is a sufficient amount to activate the locked TLL. Improvements of the buffer solution could be made from studies with tryptophan induced quenching (TrIQ) method, which is a useful tool for investigating the activation of TLL.

3.3.2 The sample preparation and setup of SE

A frozen wafer sample withstood film rupture better than an unfrozen one, but rupture of the triolein film on a solid surface in contact with aqueous solution is not disregarded in any of the two cases. The rupture depends not only on the film, but on the surface hydrophobicity. Since the used silica surface is hydrophilic, rupture by growing capillary waves can occur because of attractive van der Waals force, as reported by (Schulze H. J. et al., 2001; Michalski M. C. et al., 2000; Aarts D. A. L. et al., 2008) [31, 32, 33].

Triolein molecules saturate a hydrophilc surface with the glyceryl head groups at the surface, and the oleic acid tails facing the water solution, which is dissimilar to the conformation explained for the bulk triolein/ aqueous interface. The hydrophobic polymer, polystyrene, is layered between the hydrophilic silica surface and the triolein layer, so the triolein molecules can order themselves in the E-type conformation, with their glyceryl head groups accessible to lipase adsorption. A layer of triolein on hydrophobic silica is less stable due to nucleation happening, as explained by (Schulze H. J. et al., 2001).

The sample probably had a perforated triolein film directly when water was added to the cell, and after a 2 hour measurement, the film was no longer visible on the wafer. Filling the cell with water before putting the sample inside, could be tested as a way to minimize some film rupture.

There were repetitive malfunctions with the SE instrumentation, especially when using it after other experimental measurements had been done with different setup. This makes the preparation of the setup rather substantial, and the machine is sensitive to small changes. There was a period where the light beam had an overflow signal, so that the

integration time had to be changed from 500 ms to 1000 ms, and all the components of the instrumentation had to be restarted before every measurement. Once the positioning of X-stage and Y-stage of the machine was cleared, so the optimal position had to be reestablished, and measurements had a worse GOF-parameter during fitting after this incident.

The build up of the kinetic model had the same outset as the spectroscopic model, but could not be used due to the odd values recieved after a 2 hour measurement. Instead, measurements were performed manually and every point was fitted to a spectroscopic model. Improvements can be done on the spectroscopic model. The refractive index of an ambient is affected by ions and, to a lesser extent, by lipids, as reported by (Berlind T et al., 2008) [34]. This was not taken into account due to the ambient file being a water dispersion. In the future, a material specifically for the buffer solution should be made for the model, where the ion effect on the refractive index is included.

Complementary surface sensitive techniques can be used, but the problem of film rupture is still a subject. Spectroscopic ellipsometry is, at present, a good technique for flow measurements of a lipid layer. An optimization of the setup and the sample - ambient system could be achieved by considering the TG film rupture. Also, repetitions of measurements could exclude trends that are shown for surfaces where the lipid film has disappeared.

3.3.3 The sample preparation and setup of SAXS

The samples prepared for SAXS are yet to be investigated, since the data was noisy and no reduction of the background was made. The samples with the preparation used in this experiment, can be measured for a longer time than 3 hours to reduce noise in the data. Corroborative bulk measurements can be made with dynamic light scattering (DLS), to determine the size distribution of triolein aggregates in the sonicated samples.

4. Conclusion

There is a water uptake by the triolein oil phase, when exposed to an aqeuous solution, and it is affected by lipase activity. The activity of the active wildtype TLL and the active form of C86C255 TLL, increases the triolein layer thickness by firstly decreasing it. The inactive forms S146A and C86C255 TLL gives nearly a constant increase of the thickness of the triolein layer, but can be further discussed and compared with previous data showing that S146A TLL decreases the triolein thickness layer. The SAXS measurement shows, with limitations, that the distance between triolein molecules was greater for when active wildtype TLL was present in the aqueous solution, than in the sample with only aqueous solution and triolein. The WAXS measurement shows a more structured arrangement of the triolein molecules, when they are degraded into diglycerides, monoglycerides, glycerol and fatty acids. In closing, the lipase activity affects water uptake of the triolen phase. Spectroscopic ellipsometry studies where the lipase is added after a time of buffer exposure can be made in the future, to also see how the lipase activity is affected by the water uptake.

References

[1] Sarda, L. & Desnuelle, P. *Biochim. biophys. Acta* 30, 513–521 (1958).

[2] Barnes, G. T. & Gentle, I. R., *Interfacial Science: An Introduction*, Oxford 2011, 2nd Ed, pp. 1-2, 152-153, 257-258

[3] Lipowsky, R., Richter, D. & Kremer, K., *The Structure and Conformation of Amphiphilic Membranes*, Springer 1991, pp. 1-6

[4] Evans, D. F. & Wennerström, H., *The Colloidal Domain: Where Physics, Chemistry, Biology and Technology Meet*, Wiley 1999, pp. 14-17, 306-308, 317

[5] Tanford, C., *The hydrophobic Effect: Formation of Micelles and Biological Membranes*, Wiley 1980

[6] Sigma-Aldrich, <https://www.sigmaaldrich.com/catalog/substance/triolein88543122327l1?lang=en&region=SE>

[7] Wikipedia, by Shoyrudude555 (2007) <https://commons.wikimedia.org/wiki/File:Triolein.PNG>

[8] ChemicalBook (2017), <https://www.chemicalbook.com/ChemicalProductProperty_EN_CB5966006.htm>

[9] Bursh, T., Larsson, K. & Lundquist M., *Polymorphism in monomolecular triglyceride films on water and formation of multiomolecular films, Chem. Phys. Lipids 2*, 102-113 (1967)

[10] Hamilton, J. A., *Interactions of Triglycerides with Phospholipids: Incorporation into the Bilayer Structure and Formation of Emulsions*, Biochemistry 28, 2514-2520 (1988)

[11] Claesson, P. M. et al., *Interactions between Hydrophilic Mica Surfaces in Triolein: Triolein Surface Orientation, Solvation Forces, and Capillary Condensation*, Langmuir 13, 1682-1688 (1996)

[12] Merker, D. R. & Daubert, B.F., *The Molecular Structure in Monolayers of Saturated Triglycerides on Water as Related to Three-Dimensional Polymorphic Forms*, J. Am. Chem. Soc. 86 (6), 1009-1012 (1964)

[13] Berg, J. M. et al., *Biochemistry*, Freeman Macmillan 2015, 8th Ed, pp. 645-646, 653, 647-678

[14] Pieterson, W. A., Vidal, J. C., Volwerk, J. J. & de Haas, G. H., *Zymogen-Catalyzed Hydrolysis of Monomeric Substrates and the Presence of a Recognition Site for Lipid-Water Interfaces in Phospholipase A_2*, Biochemistry 13, 1455-1460 (1974)

[15] Willems, N. et al., *The effect of mutations in the lid region of Thermomyces lanuginosus lipase on interactions with triglyceride surfaces: A multi-scale simulation study*, Chemistry and Physics of Lipids 211, 4-15 (2018)

[16] Skjold-Jørgensen J. et al., *Understanding the activation mechanism of Thermomyces lanuginosus lipase using rational design and tryptophan-induced fluorescence quenching*, Lipid Sci. Technol. 118, 1644-1660 (2016)

[17] Derewenda, Z. S., *Structure and function of lipases*, University of Alberta, 1994, p. 10

[18] Peters, G. H. et al., *Active Serine Involved in the Stabilization of the Active Site Loop in the Humicola lanuginosa Lipase*, Biochemistry 37, 12375-12383 (1998)

[19] Liu, T. et al., *Enhancing protein stability with extended disulfide bond*s, PNAS 113 (21), 5910-5915 (2016)

[20] Durgapal, P., Ehrstein, J.R. & Nguyen, N.V., *Thin Film Ellipsometry Metrology*, AIP Conference Proceedings 449, 121 (1998)

[21] *Spectroscopic Ellipsometry User Guide,* France, HORIBA Jobin Yvon, 2008, p. 33-35

[22] Schnablegger, H. & Singh, Y., *The SAXS Guide - Getting acquainted with the principles*, Anton Paar GmbH 2013, 3rd Ed, pp. 10, 22-24, 28-29, 43, 54, 74, 89-90

[23] ResearchGate, by Lauren B McQuade (2015) <https://www.researchgate.net/figure/The-components-of-a-SAXS-instrument-including-a-typical-two-dimensional-scattering-image_fig1_279192449>

[24] Atkins, P. & de Paula, J., *Physical Chemistry*, W.H Freeman 2014, 10th Ed, p.744

[25] Stamm, A. et al., *The triolein/aqueous interface and lipase activity studied by spectroscopic ellipsometry and coarse grained simulations*, Chem Phys Lipids 211, 37-43 (2017)

[26] Skjold-Jørgensen, J. et al., *Altering the activation mechanism in Thermomyces lanuginosus lipase*, Biochemistry 53 (25), 4152-4160 (2014)

[27] Skjold-Jørgensen J. et al., *Controlled lid-opening in Thermomyces lanuginosus lipase - An engineered switch for studying lipase function*, Biophysica Acta 1865, 20-27 (2017)

[28] Dluhy, R., Cameron, D. G., Mantsch, H. H & Mendelsohn, R., *Fourier transform infrared spectroscopic studies of the effect of calcium ions on phosphatidylserine,* Biochemistry 22, 6318-6325 (1983)

[29] Spiro, T. G., *Calcium in biology*, John Wiley & Sons 1983, p.184

[30] Skjold-Jørgensen J. et al., *The enzymatic activity of lipases correlates with polarity-induced conformational changes: a trp-induced quenching fluorescence study*, Biochemistry 54, 4186-4196 (2015)

[31] Schulze H. J. et al., *The influence of acting forces on the rupture mechanism of wetting films - nucleation or capillary waves*, Colloids Surf. A Physicochem. Eng. Asp. 192, 61-72 (2001)

[32] Michalski, M. C. & Saramago B. J. V., *Static and Dynamic Wetting Behavior of Triglycerides on Solid Surfaces*, Journal of Colloid and Interface Science 227, 380-389 (2000)

[33] Aarts D. A. L. & Lekkerkerker H. N. W., *Droplet coalescence: drainage, film rupture and neck growth in uldtralow interfacial tension system*, J. Fluid Mech. 606, 275-294 (2008)

[34] Berlind. T. et al., *Effects of ion concentration on refractive indices of fluids measured by the minimum deviation technique*, Phys. stat. sol. 5, 1249-1252 (2008)